J Mater Sci: Mater Med (2011) 22:2565–2571
DOI 10.1007/s10856-011-4426-0

An approach to architecture 3D scaffold with interconnective microchannel networks inducing angiogenesis for tissue engineering

Jiaoxia Sun · Yuanliang Wang · Zhiyong Qian · Chenbo Hu

Received: 3 April 2011 / Accepted: 11 August 2011 / Published online: 23 August 2011

Abstract The angiogenesis of 3D scaffold is one of the major current limitations in clinical practice tissue engineering. The new strategy of construction 3D scaffold with microchannel circulation network may improve angiogenesis. In this study, 3D poly(D,L-lactic acid) scaffolds with controllable microchannel structures were fabricated using sacrificial sugar structures. Melt drawing sugar-fiber network produced by a modified filament spiral winding method was used to form the microchannel with adjustable diameters and porosity. This fabrication process was rapid, inexpensive, and highly scalable. The porosity, microchannel diameter, interconnectivity and surface topographies of the scaffold were characterized by scanning electron microscopy. Mechanical properties were evaluated by compression tests. The mean porosity values of the scaffolds were in the 65–78% and the scaffold exhibited microchannel structure with diameter in the 100–200 μm range. The results showed that the scaffolds exhibited an adequate porosity, interconnective microchannel network, and mechanical properties. The cell culture studies with endothelial cells (ECs) demonstrated that the scaffold allowed cells to proliferate and penetrate into the volume of the entire scaffold. Overall, these findings suggest that the fabrication process offers significant advantages and flexibility in generating a variety of non-cytotoxic tissue engineering scaffolds with controllable distributions of porosity and physical properties that could provide the necessary physical cues for ECs and further improve angiogenesis for tissue engineering.

J. Sun · Y. Wang (✉) · Z. Qian · C. Hu
Key Lab of Biorheological Science and Technology, College of Bioengineering, Ministry of Education, Research Center of Bioinspired Material Science and Engineering, Chongqing University, Chongqing 400030, China
e-mail: wyl@cqu.edu.cn

1 Introduction

Various scaffold constructs have been used for the development of tissue engineered bone; however, an active blood vessel is an essential pre-requisite for these to survive and integrate with exiting host tissue. The vascularization of the scaffold constructs is one of the major current limitations [1–4]. Vascularization within an implant is greatly increasing diffusion and allows for the optimal nutrient/waste transport for engineered tissues grown on porous scaffolds. Nevertheless, it has been demonstrated that blood vessel invasion from the host tissue in the vicinity of an engineered tissue is limited to a depth of several hundred micrometers from the surface of implant [5, 6]. Therefore, a variety of strategies have been employed to promote biomaterial vascularization such as gene and/or protein delivery of angiogenic growth factors, provision of a vascularized bone flap, and ex vivo culturing of scaffolds with Endothelial cells (ECs) alone or in combination with other cell types [7–9].

Research found that the design and architecture of the scaffold are also a critical factor for the formation of a vascular network. However, there are a limited number of methods used for the fabrication of bone tissue engineering scaffolds with the ability to form an inherent vascular network. Microfabrication of networks with vascular geometry is usually achieved by photolithography, 3D printing, or other microfabrication-based technologies [10–16], which would theoretically be able to pass oxygen and nutrients into the deeper portions of the structure and have potential to give physical cues for cell. Unfortunately, a

drawback of photolithography is its inability to create 3D architectures. 3D printing technology based on computer-aided design/computer-aided manufacturing (CAD/CAM) holds a great potential to establish an intrinsic microcapillary network. Yang et al. [16] used extrusion free forming, a rapid prototyping technique to fabricate ceramic scaffolds with three distinct structure levels: submicrometer pores, aimed to enhance cell/surface interactions, pores of tens of micrometers to encourage bone ingrowth, and corridors (100–600 μm) for vascularization. Recently, Santos et al. [17] fabricated innovation architecture, which was the nano/micro-fiber-combined scaffold. This scaffold made from a blend of starch with polycaprolactone (SPCL) having potential to elicit and guide the 3D distribution of endothelial cells. Moreover, several sacrificial techniques have been used to pattern simple microfluidic networks in scaffolds [18–20]. Bellan et al. [20] promoted the construction of a vascular network using sacrificial sugar structures. The structure was then soaked in water and the sugar-fibers solubilized leaving in the polymeric matrix macrochannels with diameters close to that of capillaries. However, the process of sacrificial sugar structure was uncontrollable.

In this study, we proposed another process for the fabrication of tissue engineering scaffolds with microchannel structures network. The microchannel structures network in the scaffold, which has potential to induce ECs ingrowth rapidly and further induce angiogenesis, would theoretically be able to pass oxygen and nutrients into the deeper portions of the structure and could provide the necessary physical cues for ECs. The basic fabrication process included two steps. First, sugar micro-fiber sacrificed scaffold was prepared by melt drawing with spiral winding. Then, this scaffold was placed into a column-like mold and added into PDLLA/methylene chloride (CH_2Cl_2) solution. After air-dry, the structure was soaked in water and the sugar-fibers solubilized leaving in the polymeric matrix macrochannels with diameters about 100 μm. The surface topography of the scaffolds, compressive properties and porosity were investigated. The capability for guiding ECs in growth was assessed with a study in vitro.

2 Experimental section

2.1 Materials

PDLLA was prepared by melt ring-opening polymerization of D,L-lactide in our laboratory initiated by stannous octoate at 140°C in vacuum, Mw = 132,000 and polydispersity = 1.44 from gel permeation chromatography with multi-angle laser light scattering (GPC-MALLS). Glucose (analytic grade), ethanol and methylene chloride (CH_2Cl_2) was obtained from Chongqing Chuandong Chemical (Group) Co., Ltd.

2.2 Preparation of sugar micro-fiber sacrificed scaffold

Sugar-fiber sacrificed scaffolds were produced by melt drawing process schematically presented in Fig. 1. The microfibers of sugar of diameters 100–200 μm were prepared using melt drawing process with a modified filament winding method. First, glucose was heated in a beaker or small vial on a hot plate until the melting point was reached. Then, keeping the temperature at 100°C until a fiber could be drawn around a mandrel that concomitantly rotates and translates sideways creating a helical and spiral trajectory for the fabrication of cylindrical structure (Fig. 1). The rotational and the translation speeds of the mandrel can be manipulated (smaller fibers for higher rotational speed, thicker fiber arrangement for lower translation speed). The technology has the capability to generate controllable radially and axially sugar sacrificed scaffold by the operating variables of the process including winding rotational and translation speeds.

2.3 Preparation of PLLA scaffold with microchannel network

The sugar sacrificed scaffold was placed into a mold (glass tube with diameter 4 cm and height 8 cm), then, 25% PDLLA/CH_2Cl_2 (w/v) was added into the mold. Expose in the air overnight so that the solvent evaporate. Then, the mold was soaked in water and the sugar-fibers solubilized leaving in the polymeric matrix microchannels with diameters about 100 μm. The water was changed about every 4 h until the sugar was totally dissolved. Finally, the scaffold was dried into vacuum desiccator.

2.4 Scaffolds morphology

The microstructures, such as microchannel size, pore distribution, and pore morphology of the scaffolds were observed by a scanning electron microscope (SEM) (Tecan Vega). The specimens were gold sputtered.

2.5 Porosity

The porosity of scaffolds was measured by the liquid displacement method [21, 22]. Ethanol is used as the displacement liquid because it can easily permeate through the scaffold. The volume of hexane was recorded as V_1, and the value of V_2 was obtained after the scaffold was immersed in ethanol for 1 h. The volume difference (V_2-V_1) was the volume of the scaffold. The ethanol impregnated scaffold was then removed from the cylinder and the residual ethanol

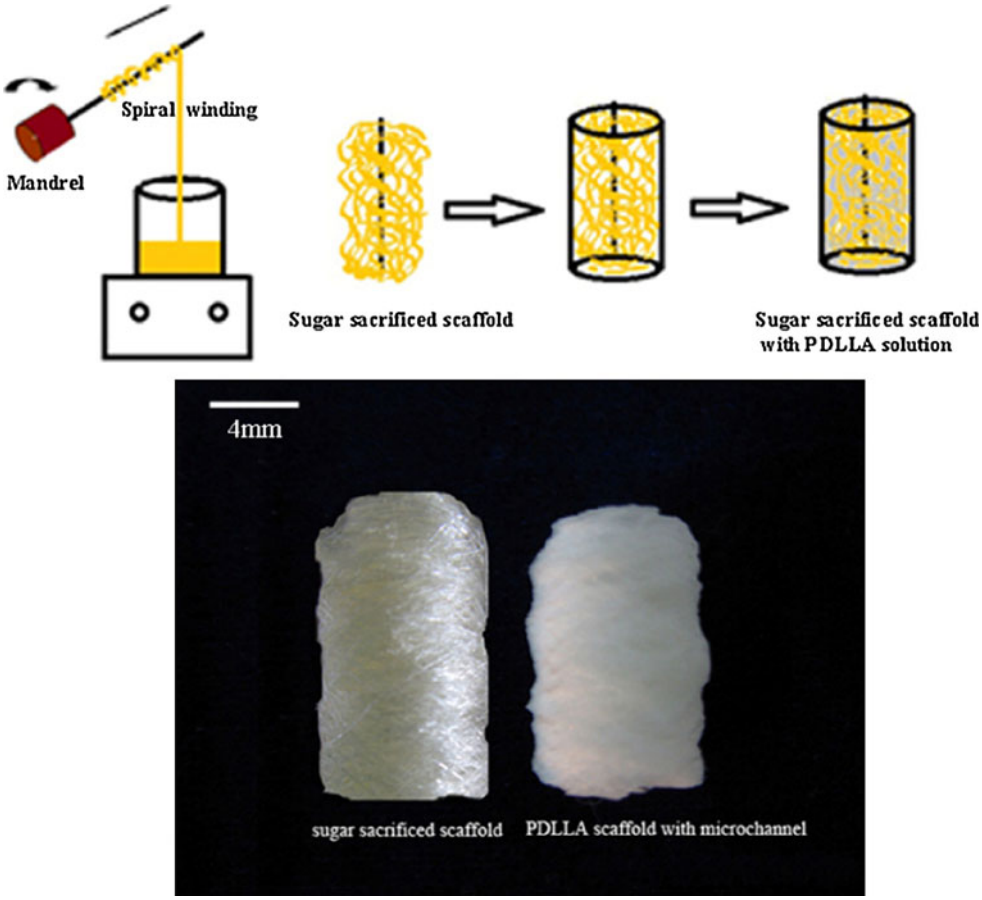

Fig. 1 The scheme of fabrication sugar sacrificed structure and scaffold

volume was recorded as V_3. The quantity (V_1-V_3), volume of ethanol within the scaffold, was determined as the void volume of the scaffold. The total volume of the scaffold was $V = (V_2 - V_1) + (V_1 - V_3) = V_2 - V_3$. The porosity of the scaffold (ε) was obtained by

$$\varepsilon\% = (V_1 - V_3)/(V_2 - V_3)100$$

2.6 Mechanical properties

The mechanical compression of the samples was evaluated on a mechanical testing equipment (Transcell Technology inc.) equipped with a 10 kN load cell at room temperature. Cylinder-shaped samples measuring 6 mm in diameter and 8 mm in height were used. The crosshead speed was 0.5 mm/min. The load was applied until the sample was compressed to 70% of its original height. The compressive strength was determined by the maximum point of the stress–strain curve. The compressive modulus was calculated as the slope of the initial linear section of the stress–strain curve.

2.6.1 Statistical analysis

All above experiments were carried out in six times. Averages and standard deviations were reported. Single factor analysis of variance (ANOVA) was performed to determine statistical significance ($P < 0.05$).

2.7 Cell, culture conditions and scaffold seeding

Endothelial cells (ECs) are generally used in tissue engineering for angiogenesis studies [23, 24]. In this study, human umbilical vein endothelial cell lines (HUVEC) were kindly provided by Chongqing medical university. The culture medium was a HEPES-buffered RPMI-1640 solution (Hyclone), supplemented with 10% fetal bovine serum, 1% penicillin and 1% streptomycin. Scaffold specimens were divided into 3 mm long sections and 6 mm diameter. They were sterilized upon being kept immersed in 75% ethanol for 2 h. The scaffolds were then washed with phosphate-buffered saline (PBS) several times to remove the ethanol, followed by exposure to UV light for 30 min following Yu et al. [25] and then pre-equilibrated with culture medium for 20 min. 100 µl containing 10^5 cells were seeded onto the surface of each scaffold and allowed to attach for 1 h at 37°C before being immersed in culture medium. The scaffolds were incubated under standard culture conditions (37°C, 5% CO_2, humidified atmosphere) for 7 days.

2.8 The localization and relative number of viable cells by MTT

To test whether cells maintained viability and grew throughout the novel scaffold live cells were identified by MTT, in which the yellow MTT solution is reduced by active mitochondria in live cells to a dark blue or purple formazan insoluble salt [26, 27]. Cell-seeded scaffolds were washed with PBS and incubated with 1 mg/ml MTT in PBS for 4 h. Then, the untransformed MTT was carefully discarded. 1 ml of dimethyl sulfoxide (DMSO, sigma) was added to the scaffold for dissolving the formazan. After 10 min, the absorbance of the solution was read on a microplate reader. The relative number of viable cells in the scaffolds was quantified by the absorbance at 490 nm.

2.9 Visualization of ECs growth on the porous scaffolds

The cell-seeded scaffolds were harvested and first washed three times with PBS (pH 7.4). Cells were fixed with 4% paraformaldehyde (mass fraction) in PBS followed by further washing. Specimen cross-section was incubated with 0.1 μl/ml of a fluorescent dye (H33238; Sigma Chemical Co., St. Louis, MO) for 10 min and PBS washing again. The distance from the specimen top surface to cross-section was 2 mm. Fluorescence images from stained samples were obtained using optical microscope (Leica). The images of cells at different locations of the scaffold were elucidated cell penetration ability.

3 Result and discussion

3.1 Structural, morphological and compressive properties of the scaffolds

The designations and the details of the processing conditions for the scaffolds of this study are provided in Table 1. The mean porosity values of the scaffolds are in the 65–78%, with the scaffolds designated as S3 exhibiting the highest porosity and S1 exhibiting the lowest (Table 1). Scaffolds for tissue engineering should possessed sufficient strength and stiffness that will bear in vivo loads so that the scaffolds can function before the growing tissue replaces the gradually degrading scaffolds matrix [28, 29]. Therefore, it is important to assess the mechanical property of the scaffold. In this study, compressive properties of the scaffold were assessed. The compressive properties are first and foremost affected by the porosity of the scaffold. The compressive modulus and the compressive yield stress of the scaffold specimens decreased with increasing porosity (Table 1). The compressive properties can be manipulated further by changing the polymer molecular weight as well as the pore size and porosity distributions [30]. Though the porosity of the scaffold is slightly lower than the scaffold by emulsion freeze-drying (85–88%), their compression modulus' (2.56–4.3 MPa) are proximity (2–4 MPa) [31]. Furthermore, these porosity values are significantly greater than the porosity values that are achieved by some other methods including sintering of microspheres (29–42% porosity) [32] and PPF scaffolds by stereolithography system (30–63%) [33].

Figure 2 shows the SEM micrographs of the samples (with designation of S3) that the translation speed of mandrel is at 0.3 m/s (Table 1), obtained upon the freeze-fracturing of the specimen in the cross-section (Fig. 2 a and b). These micrographs are characteristic of the overall interconnectivity and surface topographies of the scaffold sample. SEM micrographs reveal that the scaffold exhibits microchannel structure with diameter in the 100–200 μm range. The interconnected microchannel generating a circulation network would be able to pass oxygen and nutrients into the deeper portions of the structure. The structure could provide the necessary physical cues for ECs. Furthermore, the amplifying image (Fig. 2b) displays that the surface of the microchannel is a rough micro/nano topography, which maybe facilitate to cell attachment, migration and proliferation [34, 35].

3.2 Cell-scaffold interactions

Many traditional engineered scaffolds assured only to cells on the superficial areas because of the issue of nutrient transport; those cells growing at a greater depth in the construct face nutrient deprivation and ultimately cell death

Table 1 Scaffold designation and their various processing conditions and properties

Sample	S1	S2	S3
Rotational speed (rpm)	100	100	100
Translation speed (m/s)	0.1	0.2	0.3
Processing temperature (°C)	150−100	150−100	150−100
Porosity (%)	65.57 ± 2.20[a]	69.97 ± 1.82[a, b]	73.63 ± 1.14[b]
Compressive strength (MPa)	15.65 ± 0.59[a]	11.55 ± 0.21[a, b]	8.1 ± 0.08[b]
Compressive modulus (MPa)	4.36 ± 0.18[a]	3.31 ± 0.10[a, b]	2.62 ± 0.09[b]

[a] $P < 0.05$ for comparison between S1 and S2

[b] $P < 0.05$ for comparison between S2 and S3

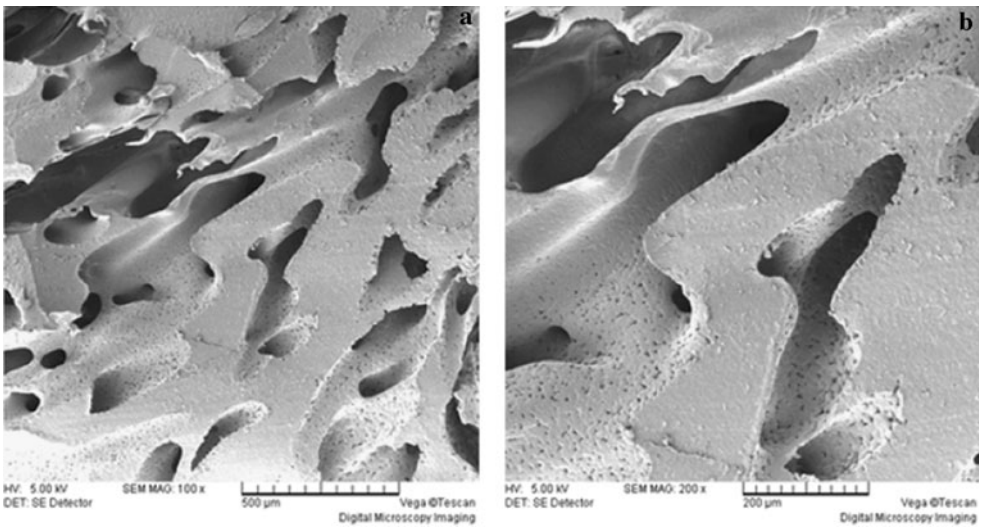

Fig. 2 Pore morphology and surface topography of scaffolds

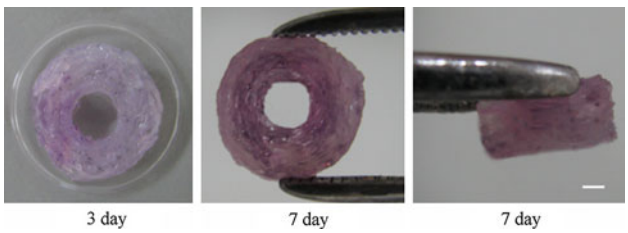

Fig. 3 At selected timepoints a scaffold was stained with MTT assay for metabolic activity, metabolically active cells were found throughout the scaffold up to day 7 of culture (Scale bar, 1 mm)

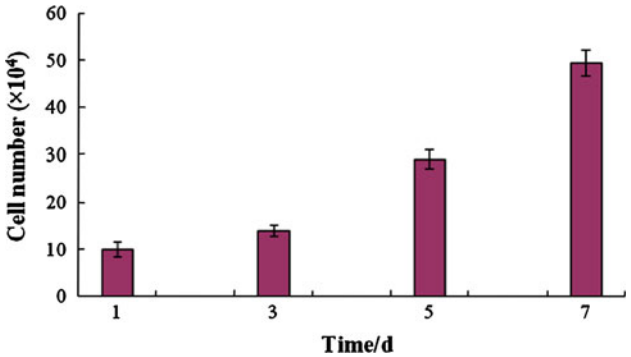

Fig. 4 MTT assay for cell proliferation on scaffold at selected timepoints

[36]. In this study, the constructed scaffold with microchannel circle network can pass oxygen and nutrients into the deeper portions of the structure, therefore, the scaffold have potential to favor cell penetration and proliferation. Cell viability, proliferation rates and location in the scaffold were assessed using the MTT assay. MTT staining shows that cells penetrated the scaffold and remained viable after 7 days of culture. The purple material in the scaffold after 7 days of culture is obviously more than 3 days of culture. And viable cells are presented throughout the scaffold (Fig. 3). Figure 4 shows that ECs proliferation rate enhanced with culture time. The proliferation rate of ECs in the first 3 days is lower than the later culture time. The possible reason is that ECs need time to adapt to the new environment. After 3 days, cells proliferate rapidly. The viability and the location of the ECs in the scaffold illustrates that the microchannel scaffolds are non-cytotoxic with favorable cell adhesion, penetration and proliferation.

Figure 5 a and b show the microscopy images of H33258 stained DNA of attached ECs cells on the cross-section of the scaffold after 3 and 7 day of culture. The fluorescence in Fig 5b is obviously stronger than in Fig 5a. Therefore, Fig. 5 a and b further confirms that the interconnectivity of porous structure of the scaffolds has indeed allowed the cells to proliferate and penetrate into the volume of the entire scaffold, which is crucial to angiogenesis.

4 Conclusions

The capabilities of a recently developed microchannel scaffolds were demonstrated. The process method was rapid, inexpensive, and highly scalable. Several processing conditions and porosities of the scaffolds were used to enable the investigation of the effects of parameters such as porosity and pore size. Using ECs it was demonstrated that the resulting functionalized microchannel scaffolds were non-cytotoxic with favorable cell adhesion, penetration and proliferation associated with the tailored distributions of porosity. The microchannel structures network in the scaffold would theoretically be able to pass oxygen and nutrients into the deeper portions of the structure and could provide the necessary physical cues for ECs rapid

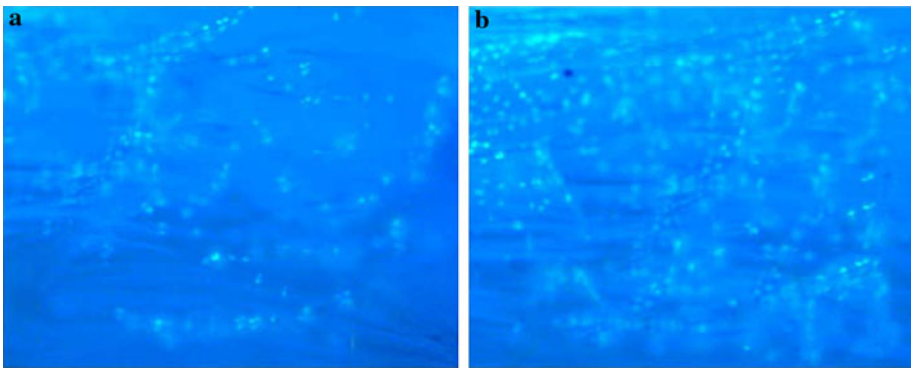

Fig. 5 Hoechst 33258 staining of the cross-section of the scaffold (S3) at day3 (**a**) and at day7 (**b**)

ingrowth. Thus, the proposed methodology is a step that is in the right direction for tissue engineering inducing angiogenesis.

Acknowledgment This study was supported by the National Natural Science Foundation of China (grant No. 30870609) and the Natural Science Foundation of Chongqing (grant No. CSTC2009 BB43821).

References

1. Kanczler JM, Oreffo RO. Osteogenesis and angiogenesis: the potential for engineering bone. Eur Cell Mater. 2008;15:100–14.
2. Laschke MW, Harder Y, Amon M, Martin I, Farhaji J, Ring A. Angiogenesis in tissue engineering: breathing life into constructed tissue substitutes. Tissue Eng. 2006;12:2093–104.
3. Shastri VP. Future of regenerative medicine: challenges and hurdles. Artif Organs. 2006;30:8282–3.
4. Santos MI, Reis RL. Vascularization in bone tissue engineering: physiology, current strategies, major hurdles and further challenges. Macromol Biosci. 2010;10:12–27.
5. Colton CK. Implantable biohybrid artificial organs. Cell Transplant. 1995;4:415–36.
6. Freshney RI. Culture of animal cells: a manual of basic techniques. New York: Wiley; 1994.
7. Koch S, Yao C, Grieb G, Prevel P, Noah EM, Steffens G. Enhancing angiogenesis in collagen matrices by covalent incorporation of VEGF. J Mater Sci Mater Med. 2006;17:735–41.
8. Richardson TP, Peters MC, Ennett AB, Mooney DJ. Polymeric system for dual growth factor delivery. Nat Biotechnol. 2001;19:1029–34.
9. Warnke PH, Springer IN, Wiltfang J, Acil Y, Eufinger H, Wehmoller M. Growth and transplantation of a custom vascularised bone graft in a man. The Lancer. 2004;364:766–70.
10. Borenstein JT, Weinberg EJ, Orrick BK, Sundback C, Kaazempur-Mofrad MR, Vacanti JP. Microfabrication of three-dimensional engineered scaffolds. Tissue Eng. 2007;13:1837.
11. Shin M, Matsuda K, Ishii O, Terai H, Kaazempur-Mofrad M, Borenstein J, Detmar M, Vacanti JP. Endothelialized networks with a vascular geometry in microfabricated poly (dimethyl siloxane). Biomed Microdevices. 2004;6:269–78.
12. Fidkowski C, Kaazempur-Mofrad MR, Borenstein J, Vacanti JP, Langer R, Wang Y. Endothelialized microvasculature based on biodegradable elastomer. Tissue Eng. 2005;11:302–9.
13. Mironov V, Boland T, Trusk T, Forgacs G, Markwald RR. Organ printing: computer-aided jet-based 3D tissue engineering. Trends Biotechnol. 2003;21:157–61.
14. Khademhosseini A, Langer R. Microengineered hydrogels for tissue engineering. Biomaterials. 2007;28:5087–92.
15. Cooke MN, Fisher JP, Dean D, Rimnac C, Mikos AG. Use of stereoliphography to manufacture critical-sized 3D biodegradable scaffolds for bone ingrowth. J Biomed Mater Res. 2003;64:65–9.
16. Yang H, Yang S, Chi X, Evans JR. Fine ceramic lattices prepared by extrusion free forming. J Biomed Mater Res. 2006;79:116–21.
17. Santos MI, Tuzlakoglu K, Fuchs S, Gomes ME, Peters K, Unger RE. Endothelial cell colonization and angiogenic potential of combined nano- and micro-fibrous scaffolds for bone tissue engineering. Biomaterials. 2008;29:4306–13.
18. Golden AP, Tien J. Fabrication of microfluidic hydrogels using molded gelatin as a sacrificial element. J Lab Chip. 2007;7:720–5.
19. Nazhat SN, Abou Neel EA, Kidane A, Ahmed I, Hope C, Kershaw M, Lee PD, Stride E, Saffari N, Knowles JC, Brown RA. Controlled microchannelling in dense collagen scaffolds by soluble phosphate glass fibers. Biomacromolecules. 2007;8:543–51.
20. Bellan LM, Singh SP, Henderson PW, Porri TJ, Craighead HG, Spector JA. Fabrication of an artificial 3-dimensional vascular network using sacrificial sugar structures. Soft Matter. 2009;5:1354–7.
21. Wan Y, Cao X, Wu Q, Zhang S, Wang S. Preparation and mechanical properties of poly (chitosan-g-DL-lactic acid) fibrous mesh scaffolds. Polym Adv Technol. 2008;19:114–23.
22. Dorati R, Colonna C, Genta I. Effect of porogen on the physicochemical properties and degradation performance of PLGA scaffolds. Polym Degrad Stabil. 2010;95:694–701.
23. Unger RE, Peters K, Huang Q, Funk A, Paul D, Kirkpatrick CJ. Vascularization and gene regulation of human endothelial cells growing on porous polyethersulfone (PES) hollow fiber membranes. Biomaterials. 2005;26:3461–9.
24. Unger RE, Peters K, Wolf M, Motta A, Mlgliarest C, Kirkpatrick CJ. Growth of human cells on a non-woven silk fibroin net: a potential for use in tissue engineering. Biomaterials. 2004;25:5137.
25. Yu X, Botchwey EA, Levine EM, Pollack SR, Laurencin CT. Bioreator-based bone tissue engineering: the influence of dynamic flow on osteoblast phenotypic expression and matrix mineralization. Proc Natl Acad Sci USA. 2004;101:11203–8.
26. Mosmann T. Rapid colorimetric assay for cellular growth and survival: application to proliferation and cytotoxicity assays. J Immunol Methods. 1983;65:55–63.
27. Ng KW, Leong DT, Hutmacher DW. The challenge to measure cell proliferation in two and three dimensions. Tissue Eng. 2005;11:182–91.
28. Cahill S, Lohfeld S, Mchugh PE. Finite element predictions compared to experimental results for the effective modulus of bone tissue engineering scaffolds fabricated by selective laser sintering. J Mater Sci Mater Med. 2009;20:1255–62.

29. Hutmacher DW. Scaffolds in tissue engineering bone and cartilage. Biomaterials. 2000;21:2529–43.
30. Karageorgiou V, Kaplan D. Porosity of 3D biomaterial scaffolds and osteogenesis. Biomaterials. 2005;26:5474–91.
31. Baker SC, Rohman G, Southgate J, Cameron NR. The relationship between the mechanical properties and cell behaviour on PLGA and PCL scaffolds for bladder tissue engineering. Biomaterials. 2009;30:1321–8.
32. Luciani A, Coccoli V, Orsi S, Ambrosio L, Netti PA. PCL microspheres based functional scaffolds by bottom-up approach with predefined microstructureal properties and release profiles. Biomaterials. 2008;29:4800–7.
33. Hollister SJ, Liao EE, Moffitt EN, Jeong CG, Kemppainen JM. In: Meyer U, editors. Fundamentals of tissue engineering and regenerative medicine. Berlin: Springer; 2009. p. 521–537.
34. Meng D, Erol M, Boccaccini AR. Processing technologies for 3D nanostructured tissue engineering scaffolds. Adv Eng Mater. 2010;9:B467–87.
35. Pattison MA, Webster TJ, Haberstroh KM. Select bladder smooth muscle cell functions were enhanced on three-dimensional, nanostructured poly(ether urethane) scaffolds. J Biomater Sci Polym Ed. 2006;17:1317–32.
36. Landman KA, Cai AQ. Cell proliferation and oxygen diffusion in a vascularising scaffold. Bull Math Biol. 2007;69:2405–28.